



Published in final edited form as:

J Immunol. 2015 November 1; 195(9): 4282–4291. doi:10.4049/jimmunol.1501220.

Differential requirements of TCR signaling in homeostatic maintenance and function of Dendritic Epidermal T Cells

Baojun Zhang^{*}, Jianxuan Wu^{*}, Yiqun Jiao[†], Cheryl Bock[‡], Meifang Dai^{*}, Benny Chen[†], Nelson Chao^{*†‡}, Weiguo Zhang^{*‡}, and Yuan Zhuang^{*‡}

^{*}Department of Immunology, Duke University Medical Center, Durham, NC 27710

[†]Department of Medicine, Duke University Medical Center, Durham, NC 27710

[‡]Duke Cancer Institute, Duke University Medical Center, Durham, NC 27710

Abstract

Dendritic Epidermal T Cells (DETCs) are generated exclusively in the fetal thymus and maintained in the skin epithelium throughout postnatal life of the mouse. DETCs have restricted antigenic specificity due to their exclusive usage of a canonical TCR. Although the importance of the TCR in DETC development has been well established, the exact role of TCR signaling in DETC homeostasis and function remains incompletely defined. Here, we investigated TCR signaling in fully matured DETCs by lineage-restricted deletion of the *Lat* gene, an essential signaling molecule downstream of the TCR. We found that *Lat* deletion impaired TCR-dependent cytokine gene activation and the ability of DETC undergoing proliferative expansion. However, LAT-deficient DETCs were able to maintain long-term population homeostasis even though with reduced proliferation rate. Mice with *Lat* deletion in DETCs exhibited delayed wound healing accompanied by impaired clonal expansion within the wound area. Our study revealed differential requirements of TCR signaling in homeostatic maintenance of DETCs and in their effector function during wound healing.

Keywords

gammadelta T cells; TCR; LAT; T cell homeostasis; Wound healing

Introduction

T cells generated in the fetal thymus represent distinct lineages that mainly become tissue resident T cells. The first wave of T cells generated in the thymus use a canonical T cell receptor (TCR) comprised of V γ 3 (alternative nomenclature V γ 5) and V δ 1 sequences,

Correspondence: Yuan Zhuang, 919-6137824, yzhuang@duke.edu.

AUTHOR CONTRIBUTIONS

BZ and YZ designed the experiments, analyzed the results and wrote the manuscript; BZ, JW and MD performed the experiments; CB cultured ES and produced knock-in mice; YJ, BC and NC collected images by two-photon microscopy and interpreted the data; WZ provided Lat^{GFP} mice and interpreted the data.

COMPETING INTERESTS STATEMENT

The authors declare no competing financial interests.

resulting in a nearly homogenous population of $\gamma\delta$ T cells(1, 2). These $\gamma\delta$ T cells migrate to the skin epidermis where they reside as a distinct population of tissue resident T cells, known as dendritic epidermal T cells (DETCs). In contrast to most circulating $\gamma\delta$ or $\alpha\beta$ T cells that are continuously generated in the postnatal thymus, DETCs maintain themselves homeostatically throughout life without additional contributions from adult hematopoietic stem cells(3, 4).

The lifelong maintenance of the DETC population is dependent on their ability to constantly communicate with the skin epithelium and self-renew under various conditions during postnatal life(4, 5). During neonatal life, the fetal derived DETCs must undergo population expansion when the surface area of skin expands at an exponential rate. DETCs in adult skin appear to proliferate in a stochastic manner at a very low rate under homeostatic conditions(6). DETCs form relatively stable dendritic structures, which make focal contacts with neighboring epithelial cells(6, 7). The constant interaction with skin epithelial cells and their ability to secrete cytokines and growth factors in response to chemical or UV induced skin damage suggest a role for DETCs in immune surveillance(2, 8, 9). Upon acute skin injury, DETCs are actively involved in wound healing process by secreting effector molecules, such as KGF and IL-17, and are able to maintain homeostasis upon wound closure(10, 11). It remains an intriguing question how DETCs keep population homeostasis while fulfilling the need to frequently respond to dynamic changes in the skin epidermis such as wound, infection, and oncogenic transformation.

TCR has been indicated to play important roles in the life and function of DETCs. Genetic studies have demonstrated that disruption of the canonical $V\gamma3V\delta1$ TCR often results in formation of DETCs with alternative TCRs of restricted clonal types (12–16). Although the selecting antigens in DETC development have not been identified, a recent study using $V\gamma3V\delta1$ DETC TCR tetramers has provided supporting evidence that antigens involved in DETC development is highly expressed in fetal thymic epithelium and wound edge(17). It has been proposed that restricted antigens are involved in selection of DETCs and activation of appropriate homing factors during DETC development(16, 18). Induced upregulation of antigens may also be responsible for activation of DETCs during wound response (17). In contrast, the role of TCR signaling in homeostatic maintenance of DETCs is less understood. Mature DETCs in the skin show hyporesponsiveness to TCR signals, suggesting a constant or frequent engagement between TCR and low dose antigens in the skin epithelium(6, 19). It has also been shown that this atypical TCR signaling mode allows DETCs to perform an immune surveillance role without triggering an immune reaction to innocuous antigens. Because the natural antigen recognized by DETC TCR is still elusive, the exact role of TCR signaling in DETC function and homeostatic maintenance remains poorly defined.

Thus far, available genetic approaches to understanding TCR function in DETCs cannot separate the TCR requirement in early T cell development from that in homeostatic maintenance. To overcome this technical hurdle, we have designed an inducible and $\gamma\delta$ T specific Cre system for lineage tracking and genetic manipulation of the tissue resident DETCs. Here, we used this newly established genetic tool to evaluate the role of TCR signaling in DETCs by deleting Linker Activation in T cell (LAT), an essential signaling

molecule downstream of TCR(20). LAT has been shown to play an essential role in the development of all T cells, including DETCs(21), and proper function, survival, and homeostatic maintenance of $\alpha\beta$ T cells(22–24). Our study showed that LAT deletion impaired the activation of DETCs in response to TCR stimulation. With disruption of TCR signaling, DETCs exhibited defects in clonal expansion during both neonatal growth and self-renewal in adult life. More importantly, impaired TCR signaling resulted in delayed wound healing accompanied by a defect in clonal expansion within the wound area. These findings identified crucial roles of TCR signaling in supporting clonal expansion of DETCs and effector function during wound healing, and suggested a redundant role in self-renewal and lifelong maintenance of the DETC population.

Materials and Methods

Mice

The *TCR δ ^{CreER}* mice were generated at the Duke Transgenic Mouse Facility. *R26^{ZsGreen}* and TCR $\gamma\delta$ KO mice were purchased from the Jackson Laboratory. *R26^{tdTomato}* mice(25) were provided by Fan Wang's lab at Duke University. Mice were bred and maintained in the SPF facility managed by Duke University Division of Laboratory Animal Research. Animal procedures were approved by the Duke University Institutional Animal Care and Use Committee.

Reagents and Flow cytometry

The antibodies used were as follows: APC/Cy7 anti-mouse CD4 (GK1.5), PB anti-mouse CD8a (53–6.7), APC anti-mouse CD19 (6D5), PE/Cy5 anti-mouse CD25 (3C7), PE anti-mouse TCR $\gamma\delta$ (GL3), PE/Cy7 anti-mouse TCR $\gamma\delta$ (GL3), PE/Cy5 anti-mouse TCR $\gamma\delta$ (GL3), PE/Cy5 anti-mouse CD3 (145-2C11), PE anti-mouse TCR γ 1.1 (2.11), PE anti-mouse TCR γ 2 (UC3–10A6), PE anti-mouse TCR γ 3 (536) and APC anti-mouse TCR β (H57–597) were purchased from Biolegend. The Cell Fixation/Permeabilization Kits, Cytometric Bead Array (CBA) kit and APC BrdU Flow Kit were from BD Biosciences. Single-cell suspensions were prepared from thymus, spleen, peripheral lymph nodes and skin, stained with Abs in the dark at 4°C for 30 min, and analyzed on a FACSCanto II flow cytometer (BD Biosciences). Flowjo software (Tree Star) was used for data analysis. Cell sorting was done on FACS Aria (BD Biosciences), MoFlo XDP (Beckman Coulter) or DIVA (BD Biosciences) sorter with the corresponding FACS software.

Epidermal DETC and dermal V γ 2 T cell preparation

Shaved skin were separated into epidermal and dermal parts after incubation with Trypsin-GNK solution (0.29% trypsin, 0.86% NaCl, 0.041% KCl and 0.1% Glucose) for 2 hours at 37°C(26–28). DETCs were isolated from epidermal sheets after incubation of the cut epidermal tissues in digestion buffer (0.27% Collagenase D, 1% DNase I, 0.01% HEPES, 0.01% Sodium pyruvate and 0.25% trypsin) on a shaker (200rpm/min) for 1–2 hour at 37°C. Dermal $\gamma\delta$ T cells were isolated by treating dermal sheets with 0.25% Trypsin, 1% DNase, 0.01% HEPES, 0.01% Sodium Pyruvate and 85 μ g/ml Liberase TM (Roche) at 37°C for 2 hours. Single cell suspension was stained with APC anti-mouse V γ 2 Ab, PE/CY7 anti-mouse TCR $\gamma\delta$ Ab and PE/CY5 anti-mouse CD3 Ab.

Microscopy

The epidermal sheets were separated from the dermal layer after 2-hour incubation in 20 mM EDTA and stained with fluorescence antibodies before image collection. The images were acquired on a Zeiss 780 confocal microscope. The whole ear scan was performed on a Zeiss 710 confocal microscope. The 3D images were taken on an Olympus multiphoton microscope. The images were processed using ImageJ and Imaris software.

Clone count

Tomato⁺ DETCs satisfying the following two criteria were considered as part of a clone. 1) Any paired Tomato⁺ DETCs are not separated by TCR δ -FITC single positive DETCs in between. 2) The distance between a paired Tomato⁺ cells is less than 62.3 μ m, which is the expected maximal distance of any two adjacent DETCs in a normal distribution ($p < 0.01$). This length is derived from the average distance of $38.0 \pm 10.4 \mu$ m obtained from randomly chosen 300 pairs of adjacent DETCs from 3 different ears with wound.

In vivo BrdU incorporation

Neonatal labeling—Newborn *TCR δ ^{CreER};Lat^{GFP/GFP}* and *Lat^{GFP/GFP}* pups were fed with 5 drops of tamoxifen (10mg/ml) daily for 5 days. At Day8 after birth, three doses of BrdU (0.3mg/mouse) were injected every other day. BrdU incorporation in DETCs was analyzed one day or 1 month after the final injection of BrdU.

Adult labeling—Young adult mice (4–6 week old) were injected i.p. by 3mg/mouse of tamoxifen over six days (1mg/mouse every other day). One week later, mice were injected with three doses of BrdU (1mg/mouse every other day). BrdU incorporation in DETCs was analyzed one day post BrdU injection. DETCs from tamoxifen and BrdU treated mice were isolated according to the published protocol (26).

TCR activation and RNA analysis

Single cells were isolated from skin epidermal sheets of *Lat^{GFP/GFP}* and *TCR δ ^{CreER};Lat^{GFP/GFP}* mice treated with tamoxifen. DETCs were sorted and stimulated by 5 μ g/ml anti-mouse CD3 Ab and 1 μ g/ml anti-mouse CD28 Ab for 24h. IL-2 production in supernatant was collected and measured using a CBA kit (BD Biosciences). IL-2 and IL-17A expression were analyzed in stimulated DETCs by intracellular staining according to Fixation/Permeabilization Kits. RNA was also extracted using RNAqueous micro kit (Life Technologies), followed by DNase I treatment. Reverse transcription was performed with M-MLV reverse transcriptase (Life Technologies). SYBR-based real-time PCR was performed to determine relative gene expression.

Wound healing model

Mice were treated with three doses of 1mg/mouse tamoxifen. After 2 weeks, full-thickness skin wounding was performed with 3mm diameter punch on the back, and wound open area was measured daily for the following 12 days(26).

Data analysis

Statistical analysis was performed using Student's t test. $P < 0.05$ was considered statistically significant as indicated in the figures.

Results

Generation of $\gamma\delta$ lineage specific Cre strain

The $TCR\delta c$ locus has been previously demonstrated to be able to drive high-level reporter expression(29). To create a $\gamma\delta$ lineage specific Cre strain, we inserted an inducible CreER expression cassette into the $TCR\delta c$ locus (Fig.1A). To test the specificity of Cre activity, we crossed $TCR\delta^{CreER}$ mice with $R26^{ZsGreen}$ reporter mice(30), in which ZsGreen expression is indicative of Cre activity (Fig.1A). We tested Cre activity by tamoxifen injection into the $TCR\delta^{CreER};R26^{ZsGreen}$ double transgenic mice. ZsGreen signal was detected in the majority of $\gamma\delta$ T cells and a small fraction of CD4 or CD8 $\alpha\beta$ T cells, but not in B cells, three days post tamoxifen treatment (Fig.1B). This result demonstrates that inducible Cre activation is highly restricted to mature $\gamma\delta$ T cells. Because the $TCR\delta c$ gene is removed upon TCR α gene rearrangement, the analysis also confirms that most $\alpha\beta$ T cells in periphery do not contain any functional $TCR\delta^{CreER}$ allele. The residual Cre activity observed in the $\alpha\beta$ T cells is most likely from recent thymic emigrants (31). Tamoxifen treatment also resulted in ZsGreen expression among $\gamma\delta$ T cells present in the thymus, lymph nodes, Peyer's patches, and liver (Fig.S1A). Time course experiments showed that reporter activation among peripheral $\gamma\delta$ T cells peaked one day post tamoxifen treatment (Fig.S1B). Ongoing thymopoiesis contributed only a small fraction of ZsGreen labeled $\gamma\delta$ T cells in the spleen or lymph nodes at later time points. Among different subsets of $\gamma\delta$ T cells, DETCs exhibited most efficient Cre activity, with more than 95% of the population expressed ZsGreen after tamoxifen treatment (Fig. 1C). The frequency of ZsGreen expression was correlated with the level of TCR expression in various subpopulations of $\gamma\delta$ T cells, confirming that Cre expression is under the transcriptional control of the $TCR\delta$ gene (Fig.S1C & D). The correlation between reporter activation and the strength of the $TCR\delta^{CreER}$ allele was also confirmed by comparing $TCR\delta^{CreER+};R26^{ZsGreen}$ mice with $TCR\delta^{CreER/CreER};R26^{ZsGreen}$ mice, where a further increase in ZsGreen labeled cells was observed in the latter group (Fig.S1E). We further analyzed Cre activation in DETCs by fluorescent microscopy. Efficient activation of the ZsGreen marker in DETCs was confirmed by the extensive overlap of ZsGreen (green) and anti-mouse TCR δ signals (red) (Fig.1D). Therefore, the $TCR\delta^{CreER}$ mice provided an effective means for lineage tracing and genetic analysis of DETCs.

Deletion of the *Lat* gene impaired TCR-mediated DETC activation

LAT is an essential adapter involved in TCR signaling pathway for both early T cell development and T cell effector function. We sought to evaluate the role of TCR signaling in DETCs by $TCR\delta^{CreER}$ -mediated deletion of the *Lat* gene. To facilitate tracking of the deletion event, we chose the *Lat^{GFP}* allele for its demonstrated utility in marking mutant T cells upon Cre-mediated deletion of *Lat*(32). Activation of the GFP marker is exclusively dependent on treatment of $TCR\delta^{CreER};Lat^{GFP/GFP}$ mice with tamoxifen (Fig.2A). Treatment of $TCR\delta^{CreER};Lat^{GFP/GFP}$ mice with tamoxifen also resulted in loss of *Lat* expression in purified DETCs in comparison with LAT-sufficient DETCs (Fig.2B). FACS analysis further

showed that over 90% of tamoxifen treated DETCs expressed GFP from the mutant allele (Fig.2C). Based on differential levels of GFP expression between the *Lat*^{GFP} heterozygous and homozygous mice, we concluded that *Lat* deletion on both chromosomes had occurred in the majority of DETCs in tamoxifen-treated *TCRδ^{CreER};Lat^{GFP/GFP}* mice (Fig.2D). In contrast to DETCs, deletion efficiency among dermal $\gamma\delta$ T cells only reached to approximately 60% after three rounds of tamoxifen treatment. The frequency of labeled cells dropped to one half after one and half month chasing due to frequent replacement from newly generated cells (Fig.2E). Under the same treatment condition, only 20% of $\gamma\delta$ T cells and 1% of $\alpha\beta$ T cells in the peripheral lymph nodes expressed GFP (Fig.2F). Therefore, this experimental system provided a relatively clean model for evaluating DETC intrinsic functions.

To investigate how LAT affects TCR signaling in DETCs, we stimulated freshly purified DETCs with anti-CD3 and anti-CD28 antibodies for 24 hours. While wild type DETCs exhibited a significant upregulation of CD69 and CD25 after prolonged TCR stimulation, LAT-deficient DETCs showed a reduced response (Fig.2G & H). Expression of CD25, CD69 and IL-2 at the transcript level were also decreased in LAT-deficient DETCs in comparison with wild type controls (Fig.2I). We further examined effector cytokine production upon TCR stimulation. Analysis of secreted IL-2 by cytometric bead array showed an impairment of IL-2 production in LAT-deficient DETCs upon TCR stimulation (Fig.2J). These data demonstrate that LAT is required for TCR-induced activation of DETCs.

DETCs maintain dendritic morphology and remain non-mobile after *Lat* deletion

The immune surveillance role of DETCs has been suggested to involve TCR signaling complexes that are highly enriched in the dendrites(6). We investigated whether LAT-mediated TCR signaling is required for the maintenance of dendrite morphology. Two-photon microscopy showed that DETCs from LAT-deficient mice had slightly lower number of dendrites than those of wild type controls ($4.73\pm 0.07/\text{cell}$ in LAT mutant vs. $5.34\pm 0.11/\text{cell}$ in wild type) (Fig.3A & B). However, dendrites from LAT-deficient DETCs were all apically anchored as previously described in wild type DETCs (Fig.3A bottom panel). Time-lapse imaging showed that both dendrites and cell bodies of LAT-deficient DETCs remained non-mobile as reported for wild type DETCs (Fig.3C and Movie S1&2). Thus LAT-mediated TCR signaling is not essential for maintaining dendrite structure, which anchors DETCs to the epithelium network.

LAT-deficient DETCs exhibited reduced proliferation rate but maintained normal population density

To evaluate TCR signaling in homeostatic proliferation and long-term maintenance of DETCs, we first compared proliferation rate between wild type and LAT-deficient DETCs in a BrdU pulse chase assay. LAT-deficient DETCs showed BrdU incorporation frequency at only $66.76\pm 13.85\%$ of that in the wild type DETCs (Fig.4A & B). We then examined the density and population size of DETCs five months post removal of the *Lat* gene. We did not detect significant differences in either cell density (Fig.4C & D) or cell numbers (Fig.4E–G) between LAT-deficient DETCs and wild type controls. Furthermore, the small number of

residual LAT-sufficient DETCs (GFP low or negative cells) in the tamoxifen treated *TCR δ ^{CreER};LAT^{GFP/GFP}* mice did not exhibit any growth advantage over time (Fig.4E). Analysis of LAT-deficient DETCs in 10-month old mice further confirmed that LAT-deficient DETCs maintained a population size indistinguishable from wild type controls (Fig.4H–J). These results indicate that although LAT controls the proliferation rate of DETCs, it is not absolutely required for long-term population maintenance of DETCs.

TCR signaling is involved in clonal expansion of DETCs during neonatal growth

DETCs are fetal derived T cells, which subsequently expand and occupy the entire skin epithelium. We found that the frequency of DETCs recovered from neonatal skin was similar to that of young adult (Fig.S2A), suggesting that the density of DETCs remains relatively constant during neonatal growth. As the surface area of skin undergoes expansion in neonatal life, DETC populations are expected to expand proportionally. We compared the growth rate between LAT-deficient DETCs and wild type DETCs by BrdU pulse labeling. Analysis of BrdU positive cells at one day or one month post labeling of neonates revealed approximately 50±15.35% or 50± 8.46% reduction, respectively, in total numbers of proliferating DETCs in LAT-deficient mice (Fig.5A–D). Similar to the adult mice, the impairment in proliferation did not result in any significant reduction in total cell numbers or density of LAT-deficient DETCs during the first month of postnatal life (Fig.S2B–D). To further evaluate the ability of individual LAT-deficient DETCs undergoing proliferative expansion, we performed a lineage tracing experiment by labeling and tracking a small number of DETCs. We combined *TCR δ ^{CreER};LAT^{GFP/GFP}* with the *R26^{tdTomato}* reporter(25), which is inefficiently activated by *TCR δ ^{CreER}* in comparison with *R26^{ZsGreen}*. Tamoxifen treatment of *TCR δ ^{CreER};LAT^{GFP/GFP};R26^{tdTomato}* mice resulted in efficient deletion of LAT but only sporadic activation of the Tomato marker (Fig.S2E & F). Importantly, all Tomato⁺ DETCs expressed high level of GFP, confirming complete deletion of the *Lat* gene among the lineage-tracked population (Fig.S2G). Under this condition, we examined the clonal size and distribution of Tomato-positive DETCs one month post tamoxifen treatment of either *TCR δ ^{CreER};R26^{tdTomato}* or *TCR δ ^{CreER};LAT^{GFP/GFP};R26^{tdTomato}* neonates. Individual clusters of Tomato-positive DETCs were detected and scored after staining of the ear epithelium sheets with FITC labeled anti-TCR δ antibody (Fig.5E & F). The majority of Tomato-positive DETCs remained as either single cells or small sized clones (less than 8 cells per cluster) for both wild type and LAT-deficient DETCs. However, a significantly higher frequency of medium to large (>9 cells per cluster) sized DETC clones were found in LAT wild type mice than in LAT-deficient mice (Fig.5F & G). Clone size of more than 16 cells was detected in 3 out of 5 LAT wild type controls but not in any of 4 LAT-deficient mice analyzed. This result indicates that TCR signaling is involved in uneven clonal expansion of DETCs at the neonatal age.

Function of DETCs in wound healing requires TCR signaling

A role for DETCs in wound healing has been demonstrated in the study of TCR δ deficient mice, in which wound healing is significantly delayed (26). However, the exact role of the TCR cannot be clearly assessed in this model due to complete removal of $\gamma\delta$ T cells at birth. Furthermore, the niche normally occupied by canonical DETCs was replaced by a different

population of dendritic T cells expressing an $\alpha\beta$ TCR in TCR δ deficient mice(12). The lineage specific and inducible deletion of LAT allowed us to evaluate TCR signaling in wound healing without disturbing the preexisting population of DETCs. We pretreated TCR $\delta^{CreER};Lat^{GFP/GFP}$ mice and *Lat*^{GFP/GFP} control mice with tamoxifen two weeks prior to the wound healing assay. After introducing a punch wound, we tracked wound size daily for 12 days. Mice with *Lat* deletion in $\gamma\delta$ T cells showed a significant delay in wound healing in comparison with the control group (Fig.6A). The degree of impairment in wound healing was similar to that reported in TCR δ deficient mice(26), which was also included in our study as a positive control.

Upon skin injury, DETCs change morphology from a dendritic to a rounded shape and subsequently enter a proliferative phase around the wound edge(6, 26). To what extent TCR signaling is involved in these sequential events is not known. We examined the dendrite structure around the wound edge within the first 10 hours following a skin cut (Fig.6B and Movie S3&4). The number of dendrites and distance to the wound edge was recorded for individual DETCs. Surprisingly, we found that LAT-deficient DETCs showed a greater loss of dendrites (Fig.6C) and a higher percentage of round or near round (1–2 dendrites/cell) morphology (Fig.S3 A & B) than the wild type controls. The average dendrite counts at the wound edge decreased 25% (from 4.65 \pm 1.48 to 3.48 \pm 1.35) for wild type DETCs in comparison with 44% (from 3.34 \pm 1.53 to 1.86 \pm 1.29,) for LAT-deficient DETCs between 0 and 10 hours post wounding (Fig.6C). This result suggests that TCR signaling may be required to stabilize the dendritic structural rather than triggering contraction in response to the wound. A persistent TCR stimulation from the dendrites during the early phase of the wound response may be necessary for DETCs to produce cytokines and growth factors before entering the proliferative phase. Indeed, time-lapse recording did not find DETC proliferation within the first 10 hours of skin cut for both genotypes (Fig.6B). TCR stimulation of LAT-deficient DETCs revealed impaired expression of genes that have been implicated in wound response(5, 11), including genes encoding Th17 pathway cytokines (Fig.S3C) and several growth factors such as KGF-1(FGF-7), KGF-2 (FGF-10), IGF-1, and TGF β 1 (Fig.S3D). Collectively, these observations support a role for TCR signaling in DETC effector function during the initial phase of wound healing.

TCR signaling is required for robust clonal expansion of DETCs around the wound edge

To evaluate the proliferative response of DETCs at the wound edge, we performed clonal analysis using the *R26^{tdTomato}* reporter described above. Mice were first treated with tamoxifen to allow stochastic activation of the tomato marker and deletion of LAT in the experimental group. One-week post treatment, a cut was made on one ear to introduce a wound edge while the other ear was left uncut as a control. To capture the initial wave of DETC proliferation, we counted Tomato-positive DETC clusters at 24 hours post wounding for both cut and uncut ears. Both wild type controls and LAT-deficient mice showed a random distribution of varying sized Tomato-positive clones across the entire ear surface of the uncut controls (Fig.S4A & B). However, examination of cut ears revealed a difference between wild type and LAT-deficient mice (Fig.7A and Fig.S4C). While the distribution of 2-cell or 3–4 cell-sized clones showed a random distribution in both genotype groups, the frequency of >4 cell-sized clones was significantly higher around the wound edge of wild

type ears ($7 \pm 2.23\%$) in comparison with all other groups (1%) (Fig. 7B & C). The appearance of clone sizes of 5–12 cells indicates the ability of DETCs to undergo at least 3–4 cell cycles within 24 hours of wounding. This result indicates that impaired TCR signaling compromised the ability of DETCs to undergo clonal expansion around the wound edge.

Discussion

TCR is an essential component for both $\alpha\beta$ and $\gamma\delta$ T cells and is absolutely required for their development and clonal selection (33). TCR-mediated signaling event is also indispensable for $\alpha\beta$ T cells to provide antigen specific immune response and homeostatic maintenance(34–37). TCR-mediated signaling in DETCs has been suggested to play multiple roles in the skin, including wound response, immune surveillance, and lifelong homeostasis(2, 38). However, due to limitations in available genetic tools, the exact role of TCR in DETC maintenance and function still remains to be fully elucidated. By combining *Lat* deletion with lineage tracking approaches, we revealed differential requirements for TCR signaling in maintaining dendritic structure, clonal expansion, and effector function during wound response and long-term homeostatic maintenance.

The TCR has been suggested to perform immune surveillance functions in DETCs by forming constitutive immunological synapses located on the dendrites of DETCs (6). Under homeostatic conditions, LAT-deficient DETCs exhibited a stable 3D dendritic morphology even though the numbers of dendrites were slightly reduced compared to wild type DETCs. Upon skin damage, DETCs normally display a rounding behavior around the wound edge(39). We found that LAT-deficient DETCs exhibited a greater degree of dendrite contraction at the wound edge than wild type controls. Our finding suggests that TCR signaling may slow down, rather than accelerate, dendrite contraction immediately after wound exposure. The delay in dendrite contraction coincided with the timing needed for TCR-mediated activation of DETCs(6). We propose that TCR signaling at the wound edge may be responsible for a delay in dendrite contraction so that DETCs have enough time to secrete cytokines and growth factors before entering proliferative phase. The rounding behavior in response to wounding is most likely regulated by other signaling events, such as NKG2D, JAML, CD100, working in parallel with TCR signals(39–42).

TCR has been shown to be required for the maintenance of naïve T cells(43–48), regulatory T cells(34, 35) and memory T cells(36, 37). In contrast, we did not see any significant change in the population size of DETCs up to 10 months with impaired TCR signaling. The slow but persistent proliferation observed in LAT-deficient DETCs indicates that DETCs could maintain their population independent of LAT-mediated TCR signals. It is important to point out that our finding is still compatible with the model that a weak and LAT-independent TCR signaling event underpins homeostatic proliferation in LAT-deficient DETCs. For example, CD6 could also initiate TCR signaling through recruiting SLP-76 and Vav1 independent of LAT(49). However, weak TCR signal alone is unlikely the main mechanism of DETC homeostasis given that most DETCs are constantly engaged in strong TCR signals. It is also possible that DETCs can proliferate at a slower rate in response to non-TCR signals, such as cytokines. Indeed the skin epidermis is known to produce IL-15, which plays an essential role in the maintenance of DETCs (50, 51). In addition to

cytokines, local IGF-1 has been shown to be involved in DETC homeostasis(10). DETCs have been shown to provide surveillance functions by sensing danger signals through NKG2D and other receptors (38, 52). It is possible that DETCs use these signaling pathways, in addition to TCR, to control homeostatic proliferation by sensing the damage or death of neighboring DETCs.

Vigorous clonal expansion is needed during neonatal growth and wound repair. It is not known whether the signal that drives clonal expansion in these growth phases is the same as the one involved in self-renewal during homeostatic maintenance. Our study clearly revealed an important role of TCR signaling in clonal expansion during both neonatal growth and wound repair, even though the same signaling event is dispensable for long-term population maintenance. This finding further supports the idea that different signals may be needed to drive robust clonal expansion versus homeostatic turnover.

Our study unequivocally demonstrated that TCR signaling is required for DETC function in wound healing. Importantly, the delay in wound healing caused by impaired TCR signaling is equivalent to that caused by complete deletion of $\gamma\delta$ T cells. Therefore, the function of DETCs in wound healing can be completely explained by TCR-mediated signaling events. Our result is consistent with the idea that DETCs regulate wound healing through TCR-mediated production of a panel of effector molecules such as KGF-1 and IL-17(11, 26). Our study also suggested that TCR-dependent clonal expansion of DETCs around the wound area could also contribute to the speed of wound healing.

Collectively, the genetic system described in our study demonstrated that TCR signaling is required for clonal expansion and effector function of DETCs. Our study also indicated that other signaling pathways, in addition to TCR signaling, is involved in lifelong homeostatic maintenance of DETCs. This system allows further investigation of candidate genes involved in various signaling pathways and thus helps better understand the regulatory mechanisms underpinning the function and lifelong homeostatic maintenance of DETCs.

Supplementary Material

Refer to Web version on PubMed Central for supplementary material.

ACKNOWLEDGEMENTS

We thank Flow Cytometry Facility of Duke Comprehensive Cancer Center for cell sorting, Duke Light Microscopy Core Facility for assistance in confocal imaging analysis, Transgenic Mouse Facility of Duke Comprehensive Cancer Center for generating $TCR\delta^{CreER}$ mice, and Dr. Fan Wang (Duke University) for sharing $R26^{tdTomato}$ mice. We thank members of the Zhuang lab and Dr. Amanda MacLeod (Duke University) for comments and suggestions.

The research described in this study has been supported by the National Institutes of Health (Grants R01GM-059638, R21RR-032742, R21AG-045440 and P01 AI102853 to Y.Z.) and the Duke University Medical Center Bridge Fund.

REFERENCES

1. Asarnow DM, Kuziel WA, Bonyhadi M, Tigelaar RE, Tucker PW, Allison JP. Limited diversity of gamma delta antigen receptor genes of Thy-1+ dendritic epidermal cells. *Cell*. 1988; 55:837–847. [PubMed: 2847872]
2. Jameson J, Havran WL. Skin gammadelta T-cell functions in homeostasis and wound healing. *Immunol Rev*. 2007; 215:114–122. [PubMed: 17291283]
3. Havran WL, Allison JP. Origin of Thy-1+ dendritic epidermal cells of adult mice from fetal thymic precursors. *Nature*. 1990; 344:68–70. [PubMed: 1968230]
4. Xiong N, Raulet DH. Development and selection of gammadelta T cells. *Immunol Rev*. 2007; 215:15–31. [PubMed: 17291276]
5. Havran WL, Jameson JM. Epidermal T cells and wound healing. *J Immunol*. 2010; 184:5423–5428. [PubMed: 20483798]
6. Chodaczek G, Papanna V, Zal MA, Zal T. Body-barrier surveillance by epidermal gammadelta TCRs. *Nature immunology*. 2012; 13:272–282. [PubMed: 22327568]
7. Havran WL, Chien YH, Allison JP. Recognition of self antigens by skin-derived T cells with invariant gamma delta antigen receptors. *Science*. 1991; 252:1430–1432. [PubMed: 1828619]
8. Girardi M, Oppenheim DE, Steele CR, Lewis JM, Glusac E, Filler R, Hobby P, Sutton B, Tigelaar RE, Hayday AC. Regulation of cutaneous malignancy by gammadelta T cells. *Science*. 2001; 294:605–609. [PubMed: 11567106]
9. MacLeod AS, Rudolph R, Corriden R, Ye I, Garijo O, Havran WL. Skin-resident T cells sense ultraviolet radiation-induced injury and contribute to DNA repair. *J Immunol*. 2014; 192:5695–5702. [PubMed: 24808367]
10. Sharp LL, Jameson JM, Cauvi G, Havran WL. Dendritic epidermal T cells regulate skin homeostasis through local production of insulin-like growth factor 1. *Nature immunology*. 2005; 6:73–79. [PubMed: 15592472]
11. MacLeod AS, Hemmers S, Garijo O, Chabod M, Mowen K, Witherden DA, Havran WL. Dendritic epidermal T cells regulate skin antimicrobial barrier function. *The Journal of clinical investigation*. 2013; 123:4364–4374. [PubMed: 24051381]
12. Jameson JM, Cauvi G, Witherden DA, Havran WL. A keratinocyte-responsive gamma delta TCR is necessary for dendritic epidermal T cell activation by damaged keratinocytes and maintenance in the epidermis. *J Immunol*. 2004; 172:3573–3579. [PubMed: 15004158]
13. Hara H, Kishihara K, Matsuzaki G, Takimoto H, Tsukiyama T, Tigelaar RE, Nomoto K. Development of dendritic epidermal T cells with a skewed diversity of gamma delta TCRs in V delta 1-deficient mice. *J Immunol*. 2000; 165:3695–3705. [PubMed: 11034374]
14. Ferrero I, Wilson A, Beermann F, Held W, MacDonald HR. T cell receptor specificity is critical for the development of epidermal gammadelta T cells. *The Journal of experimental medicine*. 2001; 194:1473–1483. [PubMed: 11714754]
15. Mallick-Wood CA, Lewis JM, Richie LI, Owen MJ, Tigelaar RE, Hayday AC. Conservation of T cell receptor conformation in epidermal gammadelta cells with disrupted primary Vgamma gene usage. *Science*. 1998; 279:1729–1733. [PubMed: 9497293]
16. Xiong N, Kang C, Raulet DH. Positive selection of dendritic epidermal gammadelta T cell precursors in the fetal thymus determines expression of skin-homing receptors. *Immunity*. 2004; 21:121–131. [PubMed: 15345225]
17. Komori HK, Witherden DA, Kelly R, Sendaydiego K, Jameson JM, Teyton L, Havran WL. Cutting edge: dendritic epidermal gammadelta T cell ligands are rapidly and locally expressed by keratinocytes following cutaneous wounding. *J Immunol*. 2012; 188:2972–2976. [PubMed: 22393149]
18. Xia M, Qi Q, Jin Y, Wiest DL, August A, Xiong N. Differential roles of IL-2-inducible T cell kinase-mediated TCR signals in tissue-specific localization and maintenance of skin intraepithelial T cells. *J Immunol*. 2010; 184:6807–6814. [PubMed: 20483745]
19. Wencker M, Turchinovich G, Di Marco Barros R, Deban L, Jandke A, Cope A, Hayday AC. Innate-like T cells straddle innate and adaptive immunity by altering antigen-receptor responsiveness. *Nature immunology*. 2014; 15:80–87. [PubMed: 24241693]

20. Finco TS, Kadlec T, Zhang W, Samelson LE, Weiss A. LAT is required for TCR-mediated activation of PLCgamma1 and the Ras pathway. *Immunity*. 1998; 9:617–626. [PubMed: 9846483]
21. Zhang W, Sommers CL, Burshtyn DN, Stebbins CC, DeJarnette JB, Tribble RP, Grinberg A, Tsay HC, Jacobs HM, Kessler CM, Long EO, Love PE, Samelson LE. Essential role of LAT in T cell development. *Immunity*. 1999; 10:323–332. [PubMed: 10204488]
22. Shen S, Chuck MI, Zhu M, Fuller DM, Yang CW, Zhang W. The importance of LAT in the activation, homeostasis, and regulatory function of T cells. *The Journal of biological chemistry*. 2010; 285:35393–35405. [PubMed: 20837489]
23. Ou-Yang CW, Zhu M, Fuller DM, Sullivan SA, Chuck MI, Ogden S, Li QJ, Zhang W. Role of LAT in the granule-mediated cytotoxicity of CD8 T cells. *Molecular and cellular biology*. 2012; 32:2674–2684. [PubMed: 22566687]
24. Ou-Yang CW, Zhu M, Sullivan SA, Fuller DM, Zhang W. The requirement of linker for activation of T cells in the primary and memory responses of CD8 T cells. *J Immunol*. 2013; 190:2938–2947. [PubMed: 23401587]
25. Wang L, Budolfson K, Wang F. Pik3c3 deletion in pyramidal neurons results in loss of synapses, extensive gliosis and progressive neurodegeneration. *Neuroscience*. 2011; 172:427–442. [PubMed: 20955765]
26. Jameson J, Ugarte K, Chen N, Yachi P, Fuchs E, Boismenu R, Havran WL. A role for skin gammadelta T cells in wound repair. *Science*. 2002; 296:747–749. [PubMed: 11976459]
27. Gray EE, Suzuki K, Cyster JG. Cutting edge: Identification of a motile IL-17-producing gammadelta T cell population in the dermis. *J Immunol*. 2011; 186:6091–6095. [PubMed: 21536803]
28. Szabo SK, Hammerberg C, Yoshida Y, Bata-Csorgo Z, Cooper KD. Identification and quantitation of interferon-gamma producing T cells in psoriatic lesions: localization to both CD4+ and CD8+ subsets. *J Invest Dermatol*. 1998; 111:1072–1078. [PubMed: 9856819]
29. Prinz I, Sansoni A, Kissenpfennig A, Ardouin L, Malissen M, Malissen B. Visualization of the earliest steps of gammadelta T cell development in the adult thymus. *Nature immunology*. 2006; 7:995–1003. [PubMed: 16878135]
30. Madisen L, Zwingman TA, Sunkin SM, Oh SW, Zariwala HA, Gu H, Ng LL, Palmiter RD, Hawrylycz MJ, Jones AR, Lein ES, Zeng H. A robust and high-throughput Cre reporting and characterization system for the whole mouse brain. *Nature neuroscience*. 2010; 13:133–140. [PubMed: 20023653]
31. Fohse L, Reinhardt A, Oberdorfer L, Schmitz S, Forster R, Malissen B, Prinz I. Differential postselection proliferation dynamics of alphabeta T cells, Foxp3+ regulatory T cells, and invariant NKT cells monitored by genetic pulse labeling. *J Immunol*. 2013; 191:2384–2392. [PubMed: 23894200]
32. Shen S, Zhu M, Lau J, Chuck M, Zhang W. The essential role of LAT in thymocyte development during transition from the double-positive to single-positive stage. *J Immunol*. 2009; 182:5596–5604. [PubMed: 19380807]
33. Ciofani M, Zuniga-Pflucker JC. Determining gammadelta versus alpha T cell development. *Nature reviews. Immunology*. 2010; 10:657–663.
34. Vahl JC, Drees C, Heger K, Heink S, Fischer JC, Nedjic J, Ohkura N, Morikawa H, Poeck H, Schallenberg S, Riess D, Hein MY, Buch T, Polic B, Schonle A, Zeiser R, Schmitt-Graff A, Kretschmer K, Klein L, Korn T, Sakaguchi S, Schmidt-Supprian M. Continuous T cell receptor signals maintain a functional regulatory T cell pool. *Immunity*. 2014; 41:722–736. [PubMed: 25464853]
35. Levine AG, Arvey A, Jin W, Rudensky AY. Continuous requirement for the TCR in regulatory T cell function. *Nature immunology*. 2014; 15:1070–1078. [PubMed: 25263123]
36. Surh CD, Sprent J. Homeostasis of naive and memory T cells. *Immunity*. 2008; 29:848–862. [PubMed: 19100699]
37. Boyman O, Letourneau S, Krieg C, Sprent J. Homeostatic proliferation and survival of naive and memory T cells. *European journal of immunology*. 2009; 39:2088–2094. [PubMed: 19637200]
38. Strid J, Tigelaar RE, Hayday AC. Skin immune surveillance by T cells--a new order? *Semin Immunol*. 2009; 21:110–120. [PubMed: 19369094]

39. Witherden DA, Watanabe M, Garijo O, Rieder SE, Sarkisyan G, Cronin SJ, Verdino P, Wilson IA, Kumanogoh A, Kikutani H, Teyton L, Fischer WH, Havran WL. The CD100 receptor interacts with its plexin B2 ligand to regulate epidermal gammadelta T cell function. *Immunity*. 2012; 37:314–325. [PubMed: 22902232]
40. Witherden DA, Verdino P, Rieder SE, Garijo O, Mills RE, Teyton L, Fischer WH, Wilson IA, Havran WL. The junctional adhesion molecule JAML is a costimulatory receptor for epithelial gammadelta T cell activation. *Science*. 2010; 329:1205–1210. [PubMed: 20813954]
41. Whang MI, Guerra N, Raulet DH. Costimulation of dendritic epidermal gammadelta T cells by a new NKG2D ligand expressed specifically in the skin. *J Immunol*. 2009; 182:4557–4564. [PubMed: 19342629]
42. Yoshida S, Mohamed RH, Kajikawa M, Koizumi J, Tanaka M, Fugo K, Otsuka N, Maenaka K, Yagita H, Chiba H, Kasahara M. Involvement of an NKG2D ligand H60c in epidermal dendritic T cell-mediated wound repair. *J Immunol*. 2012; 188:3972–3979. [PubMed: 22403443]
43. Seddon B, Zamoyska R. TCR and IL-7 receptor signals can operate independently or synergize to promote lymphopenia-induced expansion of naive T cells. *J Immunol*. 2002; 169:3752–3759. [PubMed: 12244169]
44. Brouckers T. Survival of mature CD4 T lymphocytes is dependent on major histocompatibility complex class II-expressing dendritic cells. *The Journal of experimental medicine*. 1997; 186:1223–1232. [PubMed: 9334361]
45. Kirberg J, Berns A, von Boehmer H. Peripheral T cell survival requires continual ligation of the T cell receptor to major histocompatibility complex-encoded molecules. *The Journal of experimental medicine*. 1997; 186:1269–1275. [PubMed: 9334366]
46. Kieper WC, Jameson SC. Homeostatic expansion and phenotypic conversion of naive T cells in response to self peptide/MHC ligands. *Proceedings of the National Academy of Sciences of the United States of America*. 1999; 96:13306–13311. [PubMed: 10557316]
47. Goldrath AW, Bevan MJ. Low-affinity ligands for the TCR drive proliferation of mature CD8+ T cells in lymphopenic hosts. *Immunity*. 1999; 11:183–190. [PubMed: 10485653]
48. Viret C, Wong FS, Janeway CA Jr. Designing and maintaining the mature TCR repertoire: the continuum of self-peptide:self-MHC complex recognition. *Immunity*. 1999; 10:559–568. [PubMed: 10367901]
49. Roncagalli R, Hauri S, Fiore F, Liang Y, Chen Z, Sansoni A, Kanduri K, Joly R, Malzac A, Lahdesmaki H, Lahesmaa R, Yamasaki S, Saito T, Malissen M, Aebbersold R, Gstaiger M, Malissen B. Quantitative proteomics analysis of signalosome dynamics in primary T cells identifies the surface receptor CD6 as a Lat adaptor-independent TCR signaling hub. *Nature immunology*. 2014; 15:384–392. [PubMed: 24584089]
50. De Creus A, Van Beneden K, Stevenaert F, Debacker V, Plum J, Leclercq G. Developmental and functional defects of thymic and epidermal V gamma 3 cells in IL-15-deficient and IFN regulatory factor-1-deficient mice. *J Immunol*. 2002; 168:6486–6493. [PubMed: 12055269]
51. Ye SK, Maki K, Lee HC, Ito A, Kawai K, Suzuki H, Mak TW, Chien Y, Honjo T, Ikuta K. Differential roles of cytokine receptors in the development of epidermal gamma delta T cells. *J Immunol*. 2001; 167:1929–1934. [PubMed: 11489972]
52. Strid J, Roberts SJ, Filler RB, Lewis JM, Kwong BY, Schpero W, Kaplan DH, Hayday AC, Girardi M. Acute upregulation of an NKG2D ligand promotes rapid reorganization of a local immune compartment with pleiotropic effects on carcinogenesis. *Nature immunology*. 2008; 9:146–154. [PubMed: 18176566]

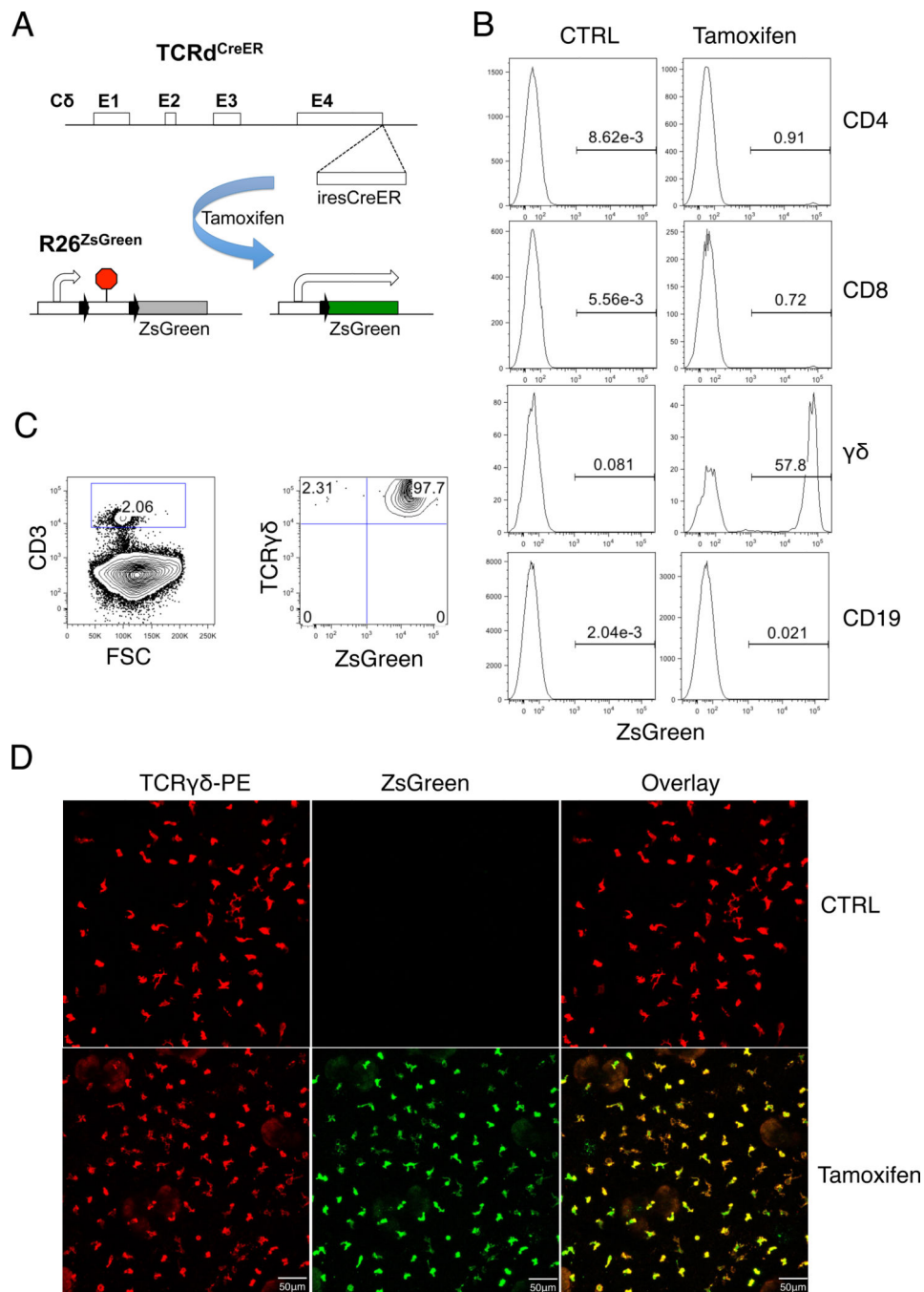


Fig. 1. Construction of $\gamma\delta$ T cell-specific and inducible Cre mouse strain
 (A) Schematic diagram of the $TCR\delta^{CreER}$ allele and strategy of Cre-mediated activation of the $R26^{ZsGreen}$. (B) FACS analysis of Cre activity in different subsets of lymphocytes. B6 WT and $TCR\delta^{CreER};R26^{ZsGreen}$ mice were intraperitoneally injected with 3 doses of 1mg/100ul tamoxifen. FACS analysis was performed three days later with fluorescently-conjugated anti-CD4, CD8, CD1d, $\gamma\delta$ and CD19 Abs. ZsGreen positive cells were shown in gated area. FACS plot is representative of n = 3 for each genotype. (C) FACS plots of ZsGreen expression in DETCs after tamoxifen treatment. DETCs were isolated from skin

epidermal sheets of mice treated with tamoxifen as in (B) and stained with PE/Cy5 labeled anti-CD3 Ab and PE/Cy7 labeled anti-TCR $\gamma\delta$ Ab. The FACS plot on the left was gated on the CD3⁺ fraction defined in the plot on the right. Each FACS plot is representative of at least 3 independent mice. (D) Representative confocal images of ZsGreen expression in skin epidermal sheets stained with PE labeled anti-TCR $\gamma\delta$ Ab. Images are representative of three mice.

Author Manuscript

Author Manuscript

Author Manuscript

Author Manuscript

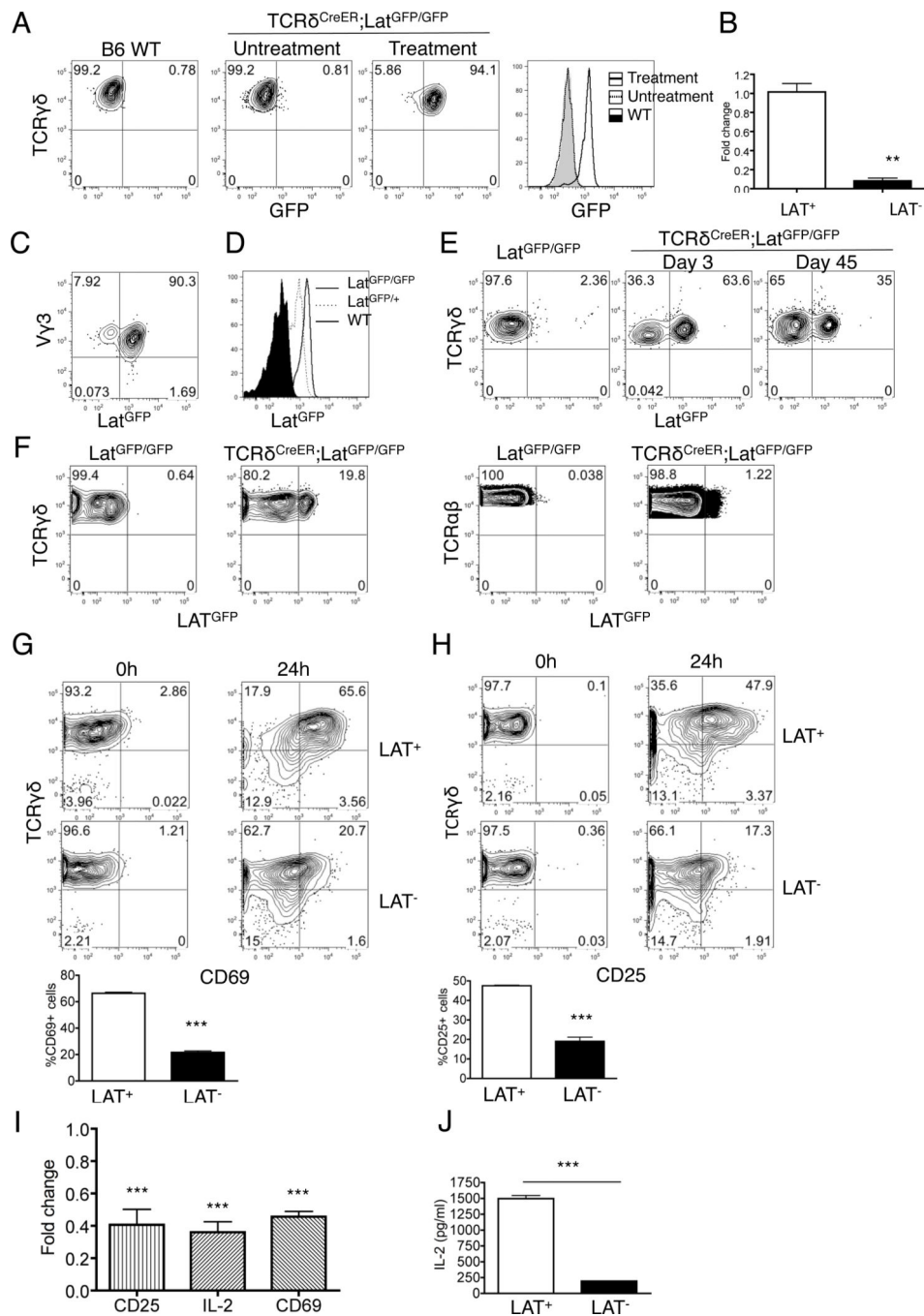


Fig. 2. Impaired TCR signaling in LAT-deficient DETCs

(A) Representative FACS analysis of GFP expression in DETCs isolated from B16 wild type mice (left panel and histogram) or *TCRδ^{CreER};Lat^{GFP/GFP}* mice either with or without three doses of tamoxifen treatment (middle panel and histogram). (B) qPCR analysis of LAT transcripts in freshly isolated DETCs from tamoxifen treated *Lat^{GFP/GFP}* (LAT⁺) and *TCRδ^{CreER};Lat^{GFP/GFP}* (LAT⁻) mice. (C) Representative FACS plot for GFP expression in Vγ3⁺ DETCs isolated from tamoxifen treated LAT⁻ mice. (D) Representative histogram for GFP expression in DETCs from either *TCRδ^{CreER};Lat^{GFP/GFP}* or *TCRδ^{CreER};Lat^{GFP/+}* mice.

(E) Representative FACS analysis of GFP expression in dermal $\gamma\delta$ T cells isolated from *Lat^{GFP/GFP}* mice (left panel) or *Lat^{GFP/GFP};TCR δ ^{CreER}* mice post tamoxifen treatment at day 3 (middle panel) or day 45 (right panel) (n=3 each). Samples have been pre-gated for V γ 2 positive cells to eliminate contaminating DETCs. (F) Representative FACS analysis of GFP expression in $\gamma\delta$ T cells and $\alpha\beta$ T cells of peripheral lymph nodes. Samples were collected two weeks post three rounds of tamoxifen injection of *Lat^{GFP/GFP}* or *TCR δ ^{CreER}Lat^{GFP/GFP}* mice. (G&H) Purified DETCs from tamoxifen treated LAT⁺ and LAT⁻ mice were stimulated by anti-CD3 and anti-CD28 Abs for 24 hours before being analyzed by FACS for CD69 (G) and CD25 (H) expression. (I&J) DETCs were isolated from *Lat^{GFP/GFP}* (LAT⁺) (n=3) and *TCR δ ^{CreER}Lat^{GFP/GFP}* (LAT⁻) (n=3) mice one week post tamoxifen treatment and stimulated with anti-CD3 and anti-CD28 antibodies for 24 hours. (I) The transcription of CD25, IL-2 and CD69 was measured by qPCR. (J) IL-2 production in supernatant was analyzed by CBA kit. *** P<0.001.

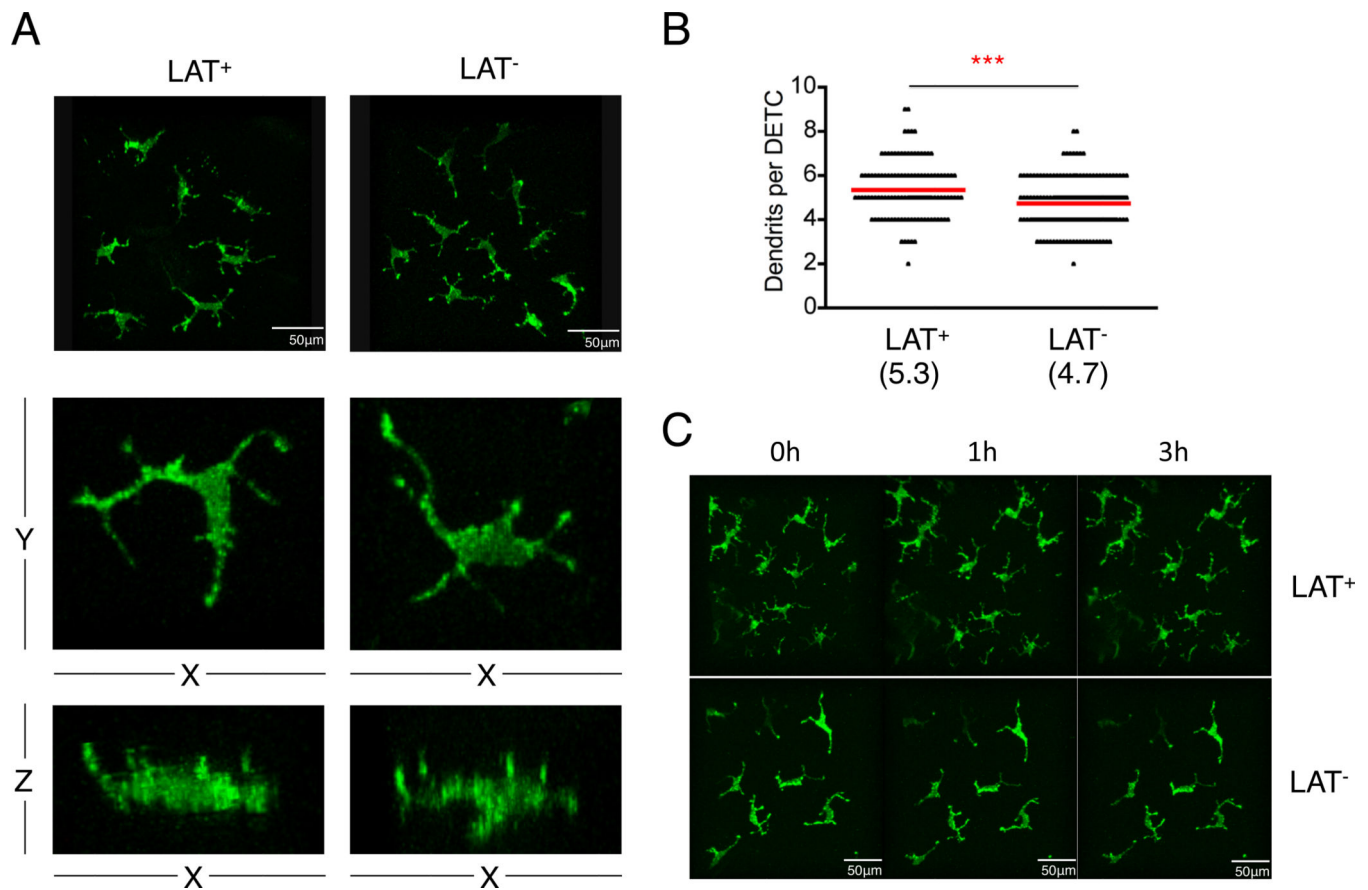


Fig. 3. Comparison of morphology and dendritic structure between LAT wild type and LAT-deficient DETCs

TCRδ^{CreER}R26^{ZsGreen} (LAT⁺) and *TCRδ^{CreER}Lat^{GFP/GFP}R26^{ZsGreen}* (LAT⁻) mice were treated with 3 doses of tamoxifen in the first week. One month later, images of DETCs were taken by two-photon microscopy. (A) Representative three-dimensional images of DETCs from indicated mice. Middle and lower panels show x-y and x-z planes of a single DETC, respectively. (B) Quantification of dendrites from DETCs of indicated mice. *** P<0.001. (C) Evaluation of DETC movement in mice with hourly intravital scans of ears for three hours. Results are representative of two independent experiments.

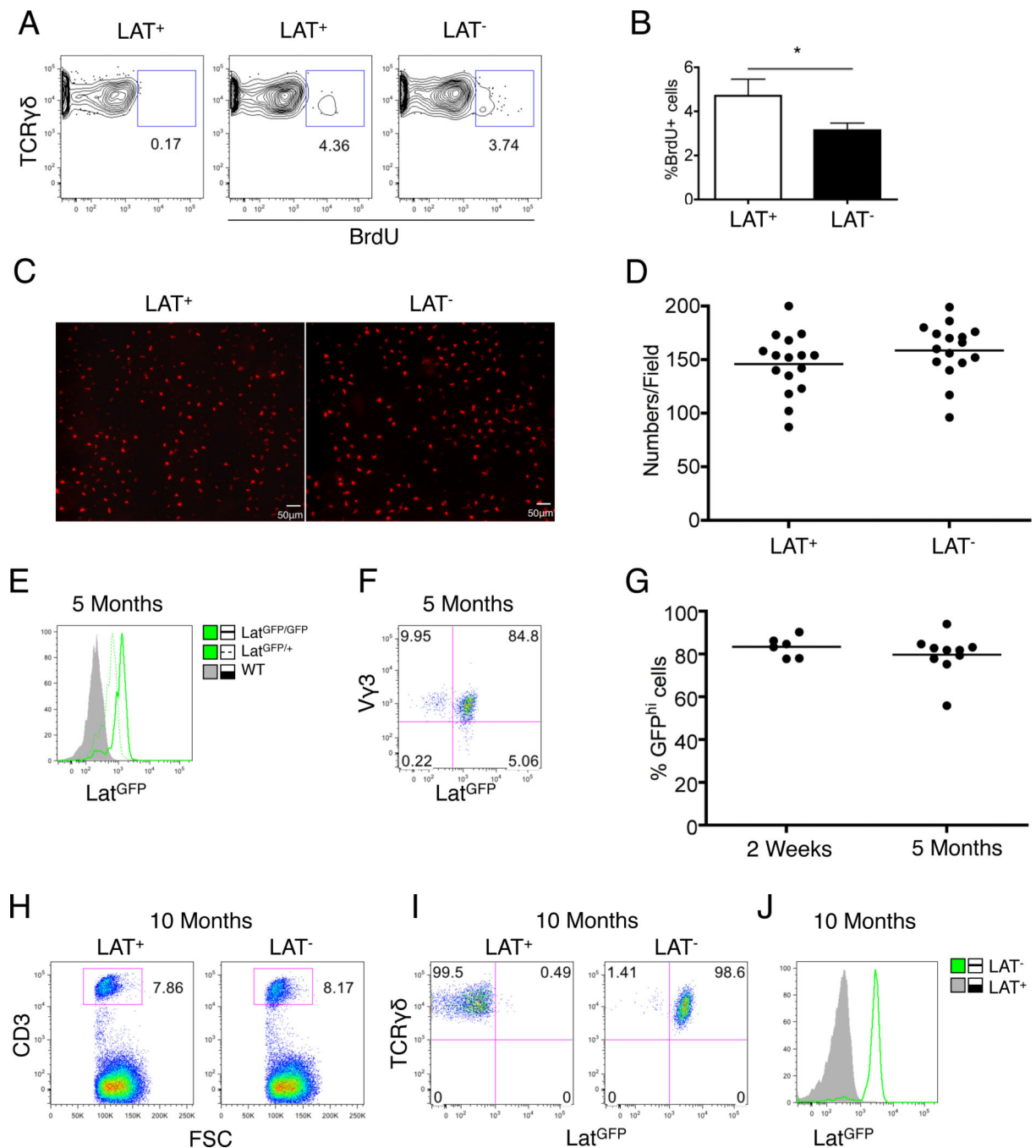


Fig. 4. LAT deficient DETCs exhibited proliferation defect but maintained long-term population homeostasis

(A) Representative FACS plots of BrdU incorporation in young adult *Lat^{GFP/GFP}* (LAT⁺) or *TCR δ ^{CreER}Lat^{GFP/GFP}* (LAT⁻) mice. DETCs were isolated and analyzed one week after tamoxifen treatment and three doses of BrdU injection. (B) Bar graph summary of (A) based on 6 mice each genotype. (C–G) LAT⁺ or LAT⁻ mice were treated with tamoxifen. Five months later, DETCs were analyzed by microscopy (C&D) or FACS (E–G). (C) Representative image analysis of DETCs. (D) DETC density from the indicated mice. Each genotype group included 16 randomly chosen areas (415 μ m \times 415 μ m/field). (E)

Representative histogram of GFP expression in DETCs from indicated mice. (F) Representative FACS plot of GFP expression in V γ 3⁺ DETCs. (G) Percentage of GFP^{hi} cells in total DETCs as defined in (F). Each dot represents a single mouse. (H) FACS gating of CD3⁺ DETCs isolated from 10-month old mice. (I) GFP and TCR γ δ expression in CD3⁺ DETCs from (H). (J) Representative histogram for GFP expression in DETCs from indicated mice. Results shown in (H–J) were based on 3 mice for each genotype.

Author Manuscript

Author Manuscript

Author Manuscript

Author Manuscript

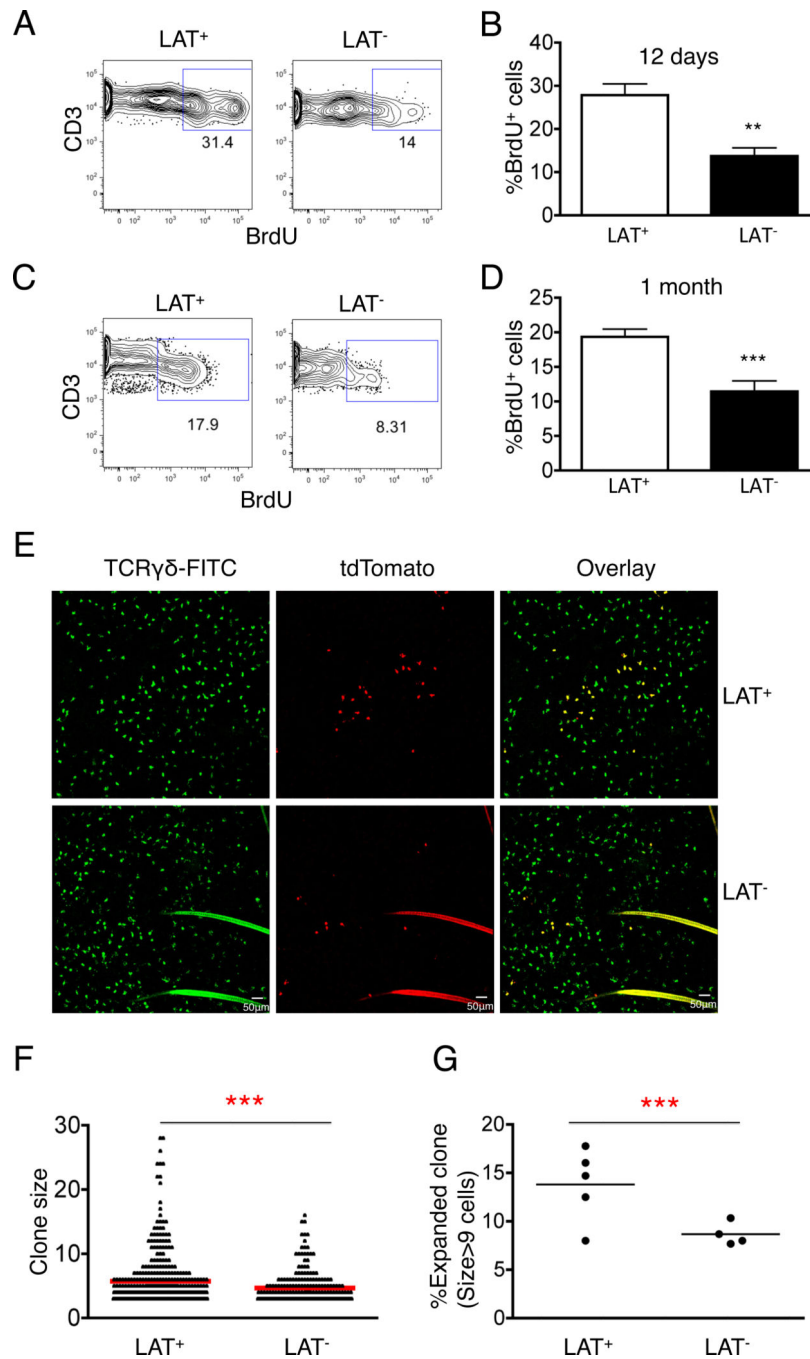


Fig. 5. Effect of TCR signaling on clonal expansion of DETCs during neonatal age
 (A&B) Representative FACS plot and bar graph summary of BrdU incorporation in DETCs at neonatal day 8 of *Lat*^{GFP/GFP} (LAT⁺) and *TCRδ*^{CreER}*Lat*^{GFP/GFP} (LAT⁻) mice. Results were based on three independent experiments. (C&D) Representative FACS plot and bar graph summary of BrdU chase labeling at one-month post neonatal BrdU injection. Results were based on three independent experiments. (E) Representative images of lineage tracked DETCs in the epidermal sheets from *TCRδ*^{CreER};*R26*^{tdTomato} (LAT⁺) and *TCRδ*^{CreER};*LAT*^{GFP/GFP};*R26*^{tdTomato} (LAT⁻) mice one month after neonatal tamoxifen

treatment. Epidermal sheets were stained with FITC labeled anti-TCR $\gamma\delta$ Ab, and all Tomato⁺ cell clusters were recorded by scanning the entire ear sheets. (F) Comparison of clonal distribution between LAT⁺ and LAT⁻ mice. Clone size larger than 2 cells were included in the graph and statistical analysis. (G) Comparison of large clone frequency (>9 cells/cluster) between LAT⁺ and LAT mice. Clone size larger than 2 cells were included in the total clone count for each mouse. Each dot indicates one mouse. Results shown in (F&G) were based on 5 *TCRd^{CreER};R26^{tdTomato}* (LAT⁺) and 4 *TCRd^{CreER};LAT^{GFP/GFP};R26^{tdTomato}* (LAT⁻) mice.

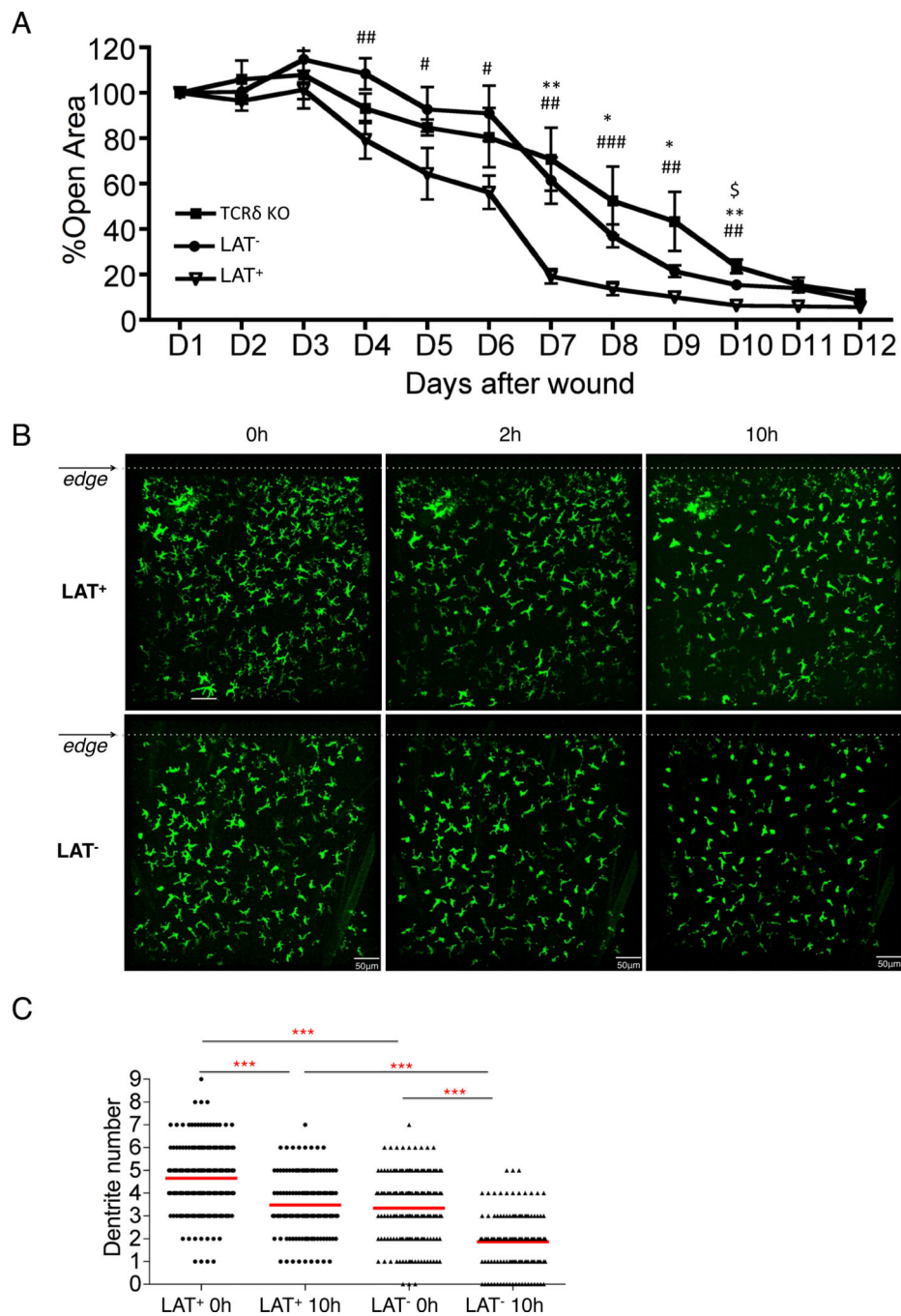


Fig. 6. Impaired wound healing upon deletion of LAT in $\gamma\delta$ T cells

(A) The kinetics of wound closure within 12 days post skin punch. Wound healing rate at each day was displayed as percentage of the wound size of Day 1 (24 hours post wounding). *, # or \$ $P < 0.05$; ** or ## $P < 0.01$; *** or ### $P < 0.001$. # represents the difference between $TCR\delta^{CreER}Lat^{GFP/GFP}$ (LAT⁻) and $Lat^{GFP/GFP}$ (LAT⁺) mice; * represents the difference between LAT⁺ and TCR δ KO mice; \$ represents the difference between LAT⁻ and TCR δ KO mice. Numbers of LAT⁺, LAT⁻, and TCR δ KO mice used in this experiment were 7, 10 and 5, respectively. (B) Representative confocal images adjacent to the wound edges (dotted

lines). Images were recorded hourly within the first 10 hours of wound punch. The images from 0, 2, and 10 hours post wounding were shown and were representative of two independent experiments. (C) Quantification of dendrite numbers of DETC within 400 μm of the wound edge. The plot shows dendrite counts of LAT⁺ DETCs at 0 hour (n=191) and 10 hour (n=138) and LAT⁻ DETCs at 0 hour (n=175) and 10 hour (n=128) post wounding. The average dendrites \pm SD for LAT⁺ at 0 hour, LAT⁺ at 10 hour, LAT⁻ at 0 hour, LAT⁻ at 10 hour are 4.65 ± 1.48 , 3.48 ± 1.35 , 3.34 ± 1.53 , 1.86 ± 1.29 , respectively. Results described in (B) and (C) were representative of 3 mice of each genotype.

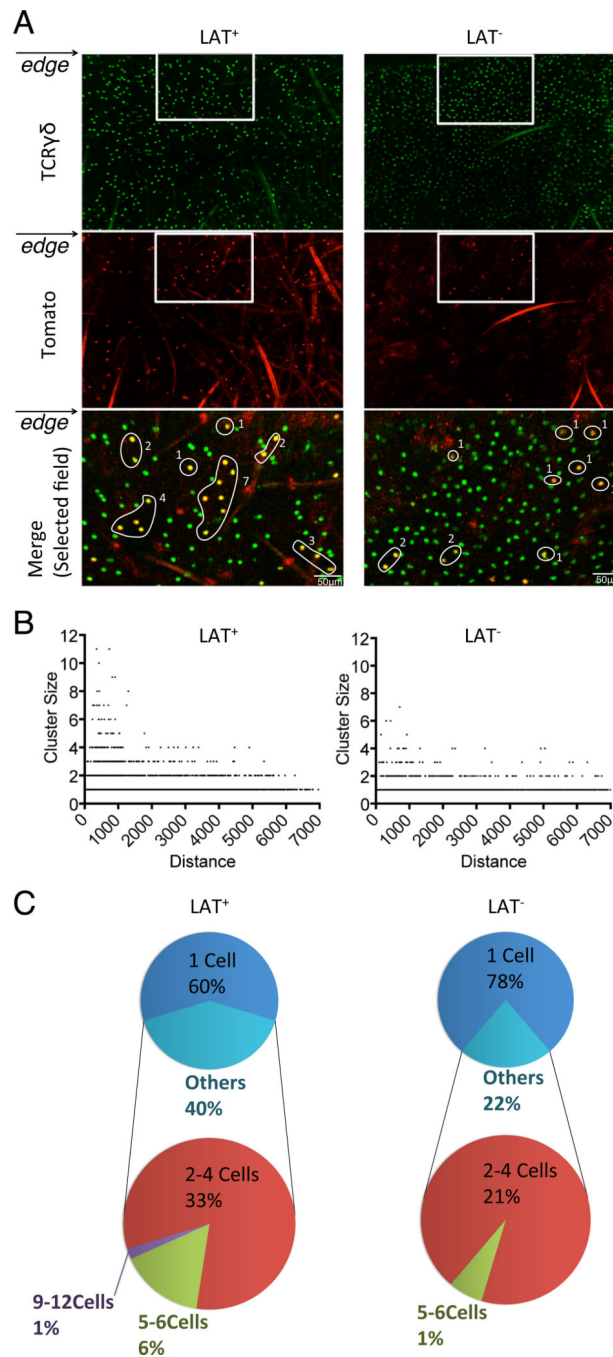


Fig. 7. Impaired clonal expansion of LAT-deficient DETCs upon wounding

(A) Representative images of DETC clones adjacent to the wound edge of *TCRd^{CreER};R26^{tdTomato}* (LAT⁺) and *TCRd^{CreER};LAT^{GFP/GFP};R26^{tdTomato}* (LAT⁻) mice at 24 hours post wounding. Merged images (bottom panel) were from the cropped areas shown in upper and middle panels. Tomato⁺ DETC clones were highlighted with circles and labeled with cell counts. (B) Correlations between clone size and distance from the wound

edge. Clone counts were based on 3 LAT⁺ and 5 LAT⁻ mice. (C) The clone distributions of DETCs within 500 μm of the wound edge. Results were based on 3 LAT⁺ and 5 LAT⁻ mice.

Author Manuscript

Author Manuscript

Author Manuscript

Author Manuscript